High Temperature, Vol. 41, No. 5, 2003, pp. 594–608. Translated from Teplofizika Vysokikh Temperatur, Vol. 41, No. 5, 2003, pp. 679–694.

PLASMA INVESTIGATIONS

The Generation of a Dense Hot Plasma by Intense Subpicosecond Laser Pulses

N. E. Andreev, M. E. Veisman, V. P. Efremov, and V. E. Fortov

Institute of High Energy Density, IVTAN (Institute of High Temperatures) Scientific Association, Russian Academy of Sciences, Moscow, 125412 Russia

Received January 8, 2003

Abstract—A simple model is developed for describing the interaction of intense femtosecond laser pulses with solid-state targets which is based on a set of equations of two-temperature hydrodynamics for electrons and ions of a plasma formed upon ionization of the target matter, equations describing the variation of ion composition of plasma upon ionization and the heat energy expenditure on thermal ionization, and equations defining the energy contribution by laser radiation to the target matter. A self-similar solution is suggested which well describes the heating of plasma electrons during the time of effect of a femtosecond laser pulse in a wide range of its parameters.

Lagrangian computer codes developed for this purpose are used to derive, in a one-dimensional approximation, a numerical solution for the set of equations for the parameters corresponding to femtosecond experimental facilities under development in Germany and Russia. Profiles of hydrodynamic quantities (electron and ion temperature, plasma pressure and density, mean ion charge) obtained in the numerical solution at different moments of time may be used for preliminary assessment of the results of future experiments with a view to optimizing their parameters.

INTRODUCTION

Extensive investigations are presently under way the world over of the interaction between matter and intense femtosecond laser pulses with an energy flux density of the order of 10^{14} W/cm^2 and higher. This is associated with both the fundamental aspects of the behavior of matter in ultrastrong laser fields and various applications such as the development of new sources of X-ray radiation, the study into the canalized propagation of laser pulses in waveguide structures, and the laser generation of shock waves. In view of this, Russian researchers are presently developing close cooperation with foreign research centers with operating femtosecond laser facilities (Israel) and with those under construction (Germany); at the same time, a Russian experimental femtosecond facility is under construction at the Institute of High Energy Density (IHED) in Moscow.

Because of serious difficulties presented by the diagnostics of the state of matter during ultrashort (femto- and picosecond) times and high material costs of such experiments, the theoretical (both analytical and numerical) methods of describing the interaction between femtosecond laser pulses and matter are gaining in importance. In the general case, the problem is very complicated, because it involves the description of the processes of absorption of the energy of laser radiation in the target matter, of optical and thermal ionization of the target matter under the effect of a laser pulse, of heating of the plasma being formed and accompanying phase transitions, of hydrodynamic flows, and of plasma radiation. For this reason, the initial stage of investigations consists in constructing models which offer the simplest way of estimating the importance of various physical phenomena occurring as a result of irradiation of a target and of estimating the parameters of plasma being formed, such as the density, temperature, pressure, and ion composition.

It is our objective to construct such models (both analytical and numerical) and use them to perform pilot investigations of the effect made on an aluminum target by laser pulses with parameters corresponding to those of femtosecond facilities under construction, DESY (Hamburg, Germany) and IHED (Moscow, Russia).

1. PHYSICAL MODEL

We will treat the following problem. A linearly polarized laser pulse with a duration of 10 fs $< t_p <$ 1 ps, peak intensity of 10^{13} W/cm$^2 \le I_{\max} < 10^{18}$ W/cm^2, and wavelength of 10 nm $< \lambda_0 <$ 10 μm. It is required to find the hydrodynamic characteristics of the plasma formed on the surface of a solid target under the effect of such a pulse, namely, the electron and ion temperature, ion composition, density, degree of expansion, and pressure. These quantities must be determined both during times of the order of laser pulse duration and during much longer times when the shock wave propagating deep into the target begins to overtake the ionization wave. In constructing simple physical models which enable one to estimate the parameters mentioned

0018-151X/03/4105-0594$25.00

above, we will proceed from the following simplifying assumptions.

It is known [1, 2] that complex processes of lattice melting and of boiling and evaporation of the liquid being formed occur when solids are affected by laser pulses of moderate peak intensity $I_{max} = 10^5$–10^{12} W/cm^2. At the same time, calculations reveal that, in the case of more intense laser pulses ($I_{max} \sim 10^{13}$–10^{14} W/cm^2), the characteristic temperature of the resultant plasma is of the order of 10 eV; in view of this, the foregoing processes may be ignored at least in a first approximation. In the case of higher laser intensities ($I_{max} \gtrsim 10^{14}$ W/cm^2), the characteristic plasma temperature turns out to be of the order of 100 eV and higher; in this case, the resultant plasma, in spite of its high density (of the order of solid-state), in a first approximation may be treated as ideal.

During the time of effect of a subpicosecond laser pulse, the plasma expands to a distance that is much less than the wavelength, so that the laser radiation is largely absorbed in the supercritical region. In so doing, subpicosecond times are not sufficient for various plasma instabilities to develop.

No electric fields are present along the gradient of plasma density in one-dimensional geometry or for an *S*-polarized laser pulse. Therefore, the generation of hot electrons may be ignored.

The basic equations of the developed physical model are given below with due regard for the foregoing.

1.1. Set of Hydrodynamic Equations

In order to describe the effect of laser radiation on solid-state targets with due regard for the processes of absorption of the energy of laser radiation, ionization, heating and scatter of the target material, and electron-ion relaxation, we will use a set of hydrodynamic equations for the total concentration of atoms and ions n_{at}, the velocity of hydrodynamic motion of quasi-neutral plasma $\mathbf{U}$, and the energy (per particle) of electrons e^{el} and ions e^{ion}, which consistently takes into account the ionization processes in matter [3],

$$\frac{\partial n_{at}}{\partial t} + \mathrm{div}(n_{at}\mathbf{U}) = 0, \tag{1}$$

$$\left[\frac{\partial}{\partial t} + \mathbf{U}\nabla\right]\mathbf{U} = -\frac{1}{\rho}\nabla[P + P^{ion}] - \frac{Zm}{4m_{ion}}K_1(\tilde{\nu})\nabla|\mathbf{V}_E|^2, \tag{2}$$

$$n\left[\frac{\partial}{\partial t} + \mathbf{U}\nabla\right]e^{el} = -\mathrm{div}\mathbf{q}_T - P\mathrm{div}\mathbf{U} - Q^{ie} + Q_{IB} + Q_J + \left[\frac{m|\mathbf{V}_E|^2}{4}K_1(\tilde{\nu}) - \frac{3}{2}T\right]S, \tag{3}$$

$$n_{at}\left[\frac{\partial}{\partial t} + \mathbf{U}\nabla\right]e^{ion} = -P^{ion}\mathrm{div}\mathbf{U} + Q^{ie}. \tag{4}$$

Here, $n_{at} = \sum_{q=0}^{z_n} n_q$, where n_q is the concentration of ions subjected to q-fold ionization (n_0 is the concentration of neutrals) and z_n is the nuclear charge. The electron concentration in the approximation of quasi-neutrality of the plasma being formed is $n = Zn_{at}$, where $Z = n_{at}^{-1}\sum_{q=1}^{z_n} q\,n_q$ is the mean ion charge. In Eqs. (1)–(4), P and P^{ion} denote the electron and ion pressure, $\rho = n_{at}m_{ion}$ is the density, and m and m_{ion} denote the electron and ion mass, respectively;

$$Q^{ie} = 3(m/m_{ion})n\nu_{ef}(T - T^{ion}) \tag{5}$$

is the density of the power transferred from electrons to ions in their collisions (electron–ion relaxation), where T and T^{ion} denote the electron and ion temperature, and ν_{ef} is the characteristic frequency of electron–ion collisions. The amplitude of oscillatory velocity of electrons in a laser field with the intensity envelope $\mathbf{E}_1$ is defined as $\mathbf{V}_E \equiv e|\mathbf{E}_1|/[m\omega_0]$, where $\omega_0 = 2\pi c/\lambda_0$ is the laser frequency. The density of inverse-bremsstrahlung heating is described by the equation

$$Q_{IB} = I_L k_0 \mathrm{Im}\{\varepsilon\}|\mathbf{E}_1/E_L|^2 = (1/2)n\nu_{ef}K_2(\tilde{\nu})m|\mathbf{V}_E|^2, \tag{6}$$

in which $k_0 = \omega_0/c$ is the vacuum wave vector of radiation, $E_L = \sqrt{8\pi I_L/c}$ is the vacuum amplitude of the field, I_L is the intensity of laser radiation, and ε is the permittivity. Expression (6) for Q_{IB} is valid in the approximation of weak spatial dispersion of permittivity, i.e., at not too high temperatures ($T < 1$ keV), when the electron-transit time in a field nonuniformity of a characteristic size is much longer than the characteristic time of electron–ion collisions $\sim\nu_{ef}^{-1}$. The functions $K_1(\tilde{\nu})$ and $K_2(\tilde{\nu})$ appearing in Eqs. (2), (3), and (6) have the form

$$K_1(\tilde{\nu}) = \frac{8}{3\sqrt{\pi}}\int_0^\infty \frac{\xi^{10}e^{-\xi^2}}{\xi^6 + \tilde{\nu}^2}d\xi,$$

$$K_2(\tilde{\nu}) \equiv 2\int_0^\infty \frac{\xi^7 e^{-\xi^2}}{\xi^6 + \tilde{\nu}^2}d\xi, \quad \tilde{\nu} = \frac{3\sqrt{\pi}}{4}\frac{\nu_{ef}}{\omega_0}.$$

The heat flux density is

$$\mathbf{q}_T = -\frac{128}{3\pi}\kappa_z\frac{nT}{m\nu_{ef}}\nabla T, \tag{7}$$

where the factor $\kappa_Z = [1 + 4.79/Z - 6.02/Z^2 + 9.13/Z^3 - 4.65/Z^4]^{-1}$ allows for the effect of electron–electron collisions on the thermal conductivity coefficient. Expres-

sion (7) implies that the heat transfer is performed by electrons. As was demonstrated by Fraenkel *et al.* [4], the radiation heat transfer may play an important part for heavy elements (under experimental conditions of [4] – BaF_2, $z_n(Ba) = 56$). The term Q_J on the right-hand side of Eq. (3) characterizes the expenditure of energy for thermal ionization,

$$Q_J = \sum_{q=1}^{q_n} [n_{q-1} W_q^{\text{th}} - n_q R_q] U_q. \quad (8)$$

Here, U_q is the q-fold ionization potential, W_q^{th} is the total frequency of q-fold thermal ionization, and R_q is the total recombination frequency. The total rate of thermal recombination in Eq. (3) is determined in the form

$$S = \sum_{q=1}^{q_n} [n_{q-1} W_q^{\text{th}} - n_q R_q]. \quad (9)$$

Set of equations (1)–(4) is derived in the approximation of relatively low intensity of the high-frequency laser field which affects matter, i.e., when the condition

$$Z|\mathbf{V}_E|^2/[1 + (\nu_{\text{ef}}/\omega_0)^2] \ll V_{\text{Te}}^2 \quad (10)$$

is valid, where $V_{\text{Te}} \equiv \sqrt{T/m}$ is the thermal velocity. This approximation is justified in the bulk of the thermal wave propagating into the target, where the field is low because of the skin effect. The violation of this approximation in the skin is taken into account by substitution of the quantity $\nu_{\text{ef}}\kappa_L$ for the effective collision frequency ν_{ef}, where

$$\kappa_L = 1 - 0.553\left[1 + 0.27 \times \frac{4T}{Zm|\mathbf{V}_E|^2}[1 + (\nu_{\text{ef}}/\omega_0)^2]^{3/4}\right]^{-1} \quad (11)$$

is Langdon's correction [5].

For closure of Eqs. (1)–(11), one must calculate the envelope of the intensity of electric field in matter $\mathbf{E}_1$, as well as determine the ionization state of the plasma being formed by calculating the quantities n_{q-1}, W_q^{th}, and R_q (see below). In addition, one must determine the form of the equations of state $P = P(n, T)$, $P^{\text{ion}} = P^{\text{ion}}(n_{\text{at}}, T^{\text{ion}})$ and $e^{\text{el}} = e^{\text{el}}(n, T)$, $e^{\text{ion}} = e^{\text{ion}}(n_{\text{at}}, T^{\text{ion}})$ and calculate the collision frequency ν_{ef}. Note that the set of equations (1)–(4) and expressions (5)–(9) for the quantities appearing in these equations are derived, strictly speaking, in the approximation of an ideal two-temperature plasma. In this case, $P = nT$, $P^{\text{ion}} = n_{\text{at}}T^{\text{ion}}$, $e^{\text{el}} = 3T/2$, $e^{\text{ion}} = 3T^{\text{ion}}/2$, and the effective frequency of electron–ion collisions ν_{ef} has the form

$$\nu_{\text{ef}} = 4\sqrt{2\pi} nZe^4\Lambda/[3\sqrt{m}T^{3/2}]. \quad (12)$$

In Eq. (12), e is the magnitude of the electron charge and Λ is the Coulomb algorithm, which may be conveniently written for a weakly nonideal plasma as

$$\Lambda = \ln\{1 + (3/\Gamma_{\text{D}})^2\}, \quad \Gamma_{\text{D}} = Ze^2/(r_{\text{De}}T),$$
$$r_{\text{De}} = \sqrt{T/(4\pi ne^2)},$$

where Γ_{D} is the Debye nonideality parameter, and r_{De} is the Debye radius.

In order to include the effects of plasma nonideality, one must first of all adjust the value of the collision frequency ν_{ef} which defines both the laser radiation energy to be absorbed (see formula (6)) and the heat flux given by Eq. (7). The effective frequency of electron–ion collisions ν_{ef} given by expression (12) increases indefinitely at $T \longrightarrow 0$ and is apparently invalid at low temperatures. At temperatures $T < 34$ eV $n_{\text{at}}/6 \times 10^{22}$ cm^{-3})$(Z/10)^{5/6}$, the electron free path $l_e \sim V_{\text{Te}}/\nu_{lf}$ ($\nu_{lf} = (3\pi/32)\nu_{\text{ef}}$ is the effective low-frequency rate of collisions, ν_{ef} is calculated by formula (12)) becomes shorter than the mean distance between ions $\bar{r} = \sqrt[3]{3/(4\pi n_{\text{at}})}$. Under these conditions, the collision frequency may be estimated by the cell model of plasma [6] as $\nu = v_{\text{av}}/[2\bar{r}]$ with $v_{\text{av}} = v(1 + \sqrt{\Gamma_{ze}})$, where v is the magnitude of the electron velocity and

$$\Gamma_{ze} = 2Ze^2/[mv^2\bar{r}] \approx 4(Z/10)^{1/6} \quad (13)$$

is the parameter of electron–ion interaction for a highly nonideal plasma. We assume that $\Gamma_{ze} \gg 1$ to derive

$$\nu \approx v\sqrt{\Gamma_{ze}}/[2\bar{r}] = \omega_{pe}/\sqrt{6}, \quad (14)$$

where $\omega_{pe} = \sqrt{4\pi ne^2/m}$ is the plasma frequency. In performing numerical calculations, the quantity $\omega_{pe}/\sqrt{6}$ was the upper limit of the electron collision frequency. In the region of even lower temperatures, i.e., below the Fermi temperature $T_F = (3\pi^2 n)^{2/3}\hbar^2/(2m)$, the following formula may be used for the effective collision frequency in a metal plasma, written in view of the effect of electron–electron collisions [7]:

$$\nu \approx \nu_0[1 + T^2/(T_F T^{\text{ion}})]; \quad \nu_0 \sim T^{\text{ion}}/\hbar, \quad (15)$$

where ν_0 is the electron–phonon collision frequency.

In addition to adjusting the expression for the collision frequency at low temperatures, one must further include the variation of the expression for the specific electron energy. At $T < T_F$, the energy $e^{\text{el}}(T) = e_{\text{met}}^{\text{el}} \equiv (\pi^2/4)T^2/T_F$. In the calculations referred to below and

performed in a wide temperature range, the following approximation expression was used:

$$e^{\mathrm{el}}(T) \approx e^{\mathrm{el}}_{\mathrm{met}} e^{\mathrm{el}}_{\mathrm{pl}} / \sqrt[3]{(e^{\mathrm{el}}_{\mathrm{met}})^3 + (e^{\mathrm{el}}_{\mathrm{pl}})^3},$$

where $e^{\mathrm{el}}_{\mathrm{pl}} \equiv 3T/2$. Note that, although the described model is rather approximate in the low-temperature region when the plasma is highly nonideal, indirect data are available which indicate that this model is capable of adequately describing both the coefficient of absorption of laser radiation in the target (see Section 1.2 below) and the heat wave propagating in the target (see Part 2). The latter fact is due to the fact that, as was demonstrated by relevant calculations, under conditions of peak intensity of laser radiation $I_{\max} > 10^{14}$ W/cm^{-3}, the electron temperature is close to or exceeds 100 eV in the bulk of the heat wave during most of the time of laser pulse effect on the target. Under these conditions, one can expect that the plasma nonideality will have an insignificant effect on the basic parameters, namely, the maximal temperature and the characteristic width of the heat wave, although it may strongly affect the shape of the leading front of the heat wave, where the plasma is always highly nonideal.

Above, we discussed the electron component of plasma. As to the ion component, because $T^{\mathrm{ion}} \ll T$, it may be highly nonideal even when the electrons are in the state of ideal gas. Nevertheless, simple reasoning reveals that the choice of equations of state for ions must not have a strong effect on the parameters of the heat wave propagating in the target, at any rate, during times less than a few picoseconds. Indeed, the absorption of laser radiation energy and the heat transfer are largely accomplished by electrons.[1] However, the time of electron–ion relaxation of energy $\Gamma_T = 2\nu_{\mathrm{ef}}^{-1} m/m_{\mathrm{ion}}$ (see formula (5)) significantly exceeds the duration of subpicosecond laser pulses; therefore, the ion energy and pressure under these conditions will be much lower than those in the case of electron gas. The foregoing is further associated with the fact that the electron concentration is Z times the ion concentration. For these reasons, the ion component has almost no effect on the electron gas energy throughout the subpicosecond laser pulse and, therefore, the exact form of the terms e^{ion} and P^{ion} is of no importance in this case. For a rough estimation of the degree of heating of the ion component, expressions corresponding to the ideal gas approximation may be used for these terms.

[1] This is characteristic of short subpicosecond laser pulses with *S*-polarized radiation. Demchenko and Rozanov [8] have demonstrated the possibility of effective absorption of energy by ions for longer *P*-polarized laser pulses, which arises under conditions of development of strong oscillation of plasma density in the neighborhood of the critical point.

1.2. Description of Absorption of Laser Radiation

To determine the density of absorbed power given by Eq. (6), one must calculate the electric field intensity. We will assume that the electric field gradient exists only in one dimension along a normal to the target surface (x axis); this presumes a not too sharply focused laser pulse whose transverse dimension exceeds the characteristic longitudinal dimension of the region of field localization (as a rule, ten nanometers or less). We will assume the laser pulse is *S*-polarized and incident on the target surface at an angle θ to its normal. In this case, assuming the spatial dispersion is small, we will find that the envelope of the electric field intensity $\mathbf{E}_1 = \mathbf{e}_y E$ is determined from the solution of the problem

$$\begin{gathered} \partial^2 E/\partial x^2 + k_0^2[\varepsilon(x) - \sin^2(\theta)]E(x) = 0, \\ \partial E/\partial x(x = +0) = [2E_L - E(x = +0)]ik_0\cos(\theta); \\ E(x = \infty) = 0. \end{gathered} \tag{16}$$

Here, the permittivity ε for an ideal plasma is described by the expression

$$\begin{gathered} \varepsilon(x) = 1 - [n(x)/n_c][K_1(\tilde{\nu}(x)) \\ - i(\nu_{\mathrm{ef}}(x)/\omega_0)K_2(\tilde{\nu}(x))]. \end{gathered} \tag{17}$$

The functions K_1 and K_2 determined in Section 1.1 exhibit the asymptotic behavior $K_1(\tilde{\nu} \longrightarrow 0) = K_2(\tilde{\nu} \longrightarrow 0) = 1$ and $K_1(\tilde{\nu} \longrightarrow \infty) \sim (315/8)/\tilde{\nu}^2$, $K_2(\tilde{\nu} \longrightarrow \infty) \sim 6/\tilde{\nu}^2$, where formula (17) reduces to the well-known cases for the normal high-frequency and normal low-frequency skin effects, respectively. For a metal, the permittivity is found by the Drude phenomenological formula,

$$\varepsilon(x) = 1 - [n(x)/n_c]/[1 + i(\nu(x)/\omega_0)] \tag{18}$$

with the frequency ν calculated by formula (15), where $n_c = n\omega_0^2/[4\pi e^2]$ is the critical concentration. The approximation transforming to formulas (17) and (18) in the extreme cases is used in the intermediate region.

Equations (16) may be used to find the absorption coefficient $A = 1 - I_r/I_L$ (I_r is the intensity of radiation reflected from the target),

$$A = (k_0/\cos(\theta))\int_0^\infty \mathrm{Im}\{\varepsilon(x)\}|E(x)/E_L|^2 dx. \tag{19}$$

This quantity may also be found from the conditions of continuity on the plasma–vacuum interface of the tangential components of electric and magnetic fields as

$$\begin{gathered} A = 4\cos(\theta)\mathrm{Re}\{\zeta\}|\zeta\cos(\theta) + 1|^{-2}, \\ \zeta = ik_0[\partial \ln E/\partial x]^{-1}\big|_{x = +0}, \end{gathered} \tag{20}$$

where ζ is the impedance dependent on the field distribution $E(x > 0)$ within the plasma. Comparison of the results of calculation of A by formulas (19) and (20)

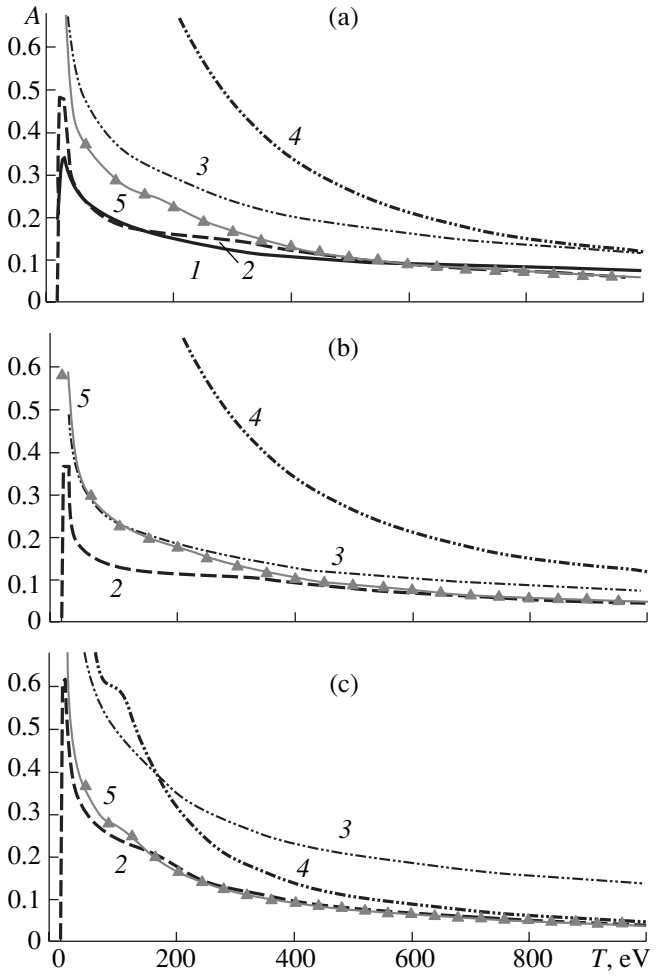

Fig. 1. The absorption coefficient A of an aluminum plasma with a stepped boundary as a function of electron temperature T: (a) $\lambda_0 = 0.4$ μm, normal density; (b) $\lambda_0 = 1.06$ μm, normal density; (c) $\lambda_0 = 0.4$ μm, 0.1 normal density; (*1*) results of [9]; (*2*) model (20), (21), (17), (18); (*3*, *4*) approximation (23), *3* – $\tilde{\nu} \gg 1$, *4* – $\tilde{\nu} \ll 1$; (*5*) approximation (24).

enables one to check the accuracy of the numerical solution of wave equation (16).

Under conditions of a weak spatial dispersion for a homogeneous plasma with a stepped density profile, the impedance may be calculated by the formula

$$\zeta = 1/\sqrt{\varepsilon - \sin^2(\theta)}. \tag{21}$$

We substitute the permittivity given by Eq. (17) into (21) to derive from formula (20) the following expression for the absorption coefficient of a hot plasma of solid-state density with the electron concentration $n \gg n_c$:

$$A = \cos(\theta)2\sqrt{2}(\omega_0/\omega_{pe})\sqrt{K_3 - K_1}/K_3, \qquad K_3 \equiv \sqrt{K_1^2 + \tilde{\nu}^2 K_2^2}. \tag{22}$$

In two extreme cases of *normal low-frequency* skin effect at $\tilde{\nu} \gg 1$ and *normal low-frequency* skin effect at $\tilde{\nu} \ll 1$, it follows from Eqs. (22) that

$$A = \begin{cases} \cos(\theta)\sqrt{8\omega_0\nu_{lf}}/\omega_{pe}, & \nu_{lf} = (3\pi/32)\nu_{\text{ef}} \\ \tilde{\nu} \gg 1 \\ \cos(\theta)2\nu_{\text{ef}}/\omega_{pe}, & \tilde{\nu} \ll 1. \end{cases} \tag{23}$$

Figure 1 gives, for a homogeneous aluminum plasma, the results of calculation of the absorption coefficient A of normally incident ($\theta = 0$) laser radiation by the aforementioned model (20), (21) under conditions of normal skin effect (i.e., disregarding the spatial dispersion) with the permittivity given by Eqs. (17) and (18) in the region of degenerate plasma and with the collision frequency determined in the respective regions by formulas (12), (14), and (15). The results of a more exact calculation in view of the spatial dispersion and absorption in a nonideal plasma, borrowed from [9], and analytical approximations (23) are also given in Fig. 1. The value of the average ion charge was calculated by the Saha model with a "cut-off" (see Section 1.3).

The results of comparison of curves in Fig. 1a lead one to conclude that the suggested simple model adequately describes the absorption coefficient in a wide temperature range. Respective estimates (see, for example, [3]) demonstrate that the collisionless absorption in modes, where the spatial dispersion is significant (the so-called modes of sheet-inverse-bremsstrahlung and anomalous skin effects, see [3]), in the case of short-wave laser pulses becomes significant only at rather high temperatures in the vicinity of 1 keV. The inclusion of collisionless absorption at high temperatures in the calculation [9] leads to somewhat higher values of the absorption coefficient compared to those obtained by the model described in Section 1.2 (see the solid and dashed curves in Fig. 1a at $T > 800$ eV).

The calculation results in Fig. 1a further demonstrate that the limiting formulas (23) extensively used in the literature produce an inadequate accuracy of calculation of the absorption coefficients for the parameters of the problem being treated. However, the use of the approximation formula

$$A = 0.5\kappa_A\sqrt{A_{lf}A_{hf}}, \tag{24}$$

where A_{lf} and A_{hf} are the limiting absorption coefficients of Eq. (23) at $\tilde{\nu} \gg 1$ and $\tilde{\nu} \ll 1$, respectively, enables one to adequately describe the absorption coefficients in a wide range of parameters of the problem (see Fig. 1).

In formula (24), the parameter κ_A is the so-called variation factor of absorption. It is equal to the ratio of the absorption coefficient for an expanding inhomogeneous plasma of the target being irradiated, when the nonlinear field dependence of absorption is taken into account using the Langdon correction (11), to the field-

linear absorption coefficient for a homogeneous semi-infinite plasma of the same maximal temperature and solid-state density. The data in Fig. 1 were obtained with the coefficient $\kappa_A = 1$. For a real plasma formed on the surface of a solid-state target irradiated by a laser pulse of an intensity in excess of 10^{14} W/cm^2, the coefficient κ_A weakly depends on time at $t > 10$ fs and may be taken to be $\kappa_A \approx 0.4$ (see [3]). The fact that, for an expanding plasma and/or significant values of laser intensity, $\kappa_A < 1$ is associated with the decrease in absorption due to a decrease in the effective collision frequency because of a drop of the plasma density (expansion) or because of the presence of the Langdon correction (11). Note that the choice of the coefficient κ_A further enables one to take into account the fact that it is not the entire energy of laser radiation that converts to the energy of thermal motion of electrons: a significant part of the absorbed energy transforms to the energy of hydrodynamic motion of plasma and is spent to perform ionization [3, 10].

1.3. Description of Ionization of Matter

The dynamics of heating and energy transport in a plasma formed upon stimulation of a target by an intense laser pulse largely depends on the average ion charge which affects the kinetic coefficients. In addition, the expenditure of energy to ionize matter may affect the distribution of absorbed energy in matter. This defines the need for self-consistent inclusion of ionization processes in describing the effect of radiation on matter.

In order to determine the quantities S, Q_J, and Z entering Eqs. (2) and (3), one needs to calculate the total ionization frequencies W_q^{th}, the total recombination frequencies R_q, and the concentrations n_{q-1} of ions with the degree of ionization $q - 1$. Equations for n_q may be written as

$$\partial n_q/\partial t + \operatorname{div}(n_q \mathbf{U}) = S_q^{\text{th}}, \tag{25}$$

$$S_q^{\text{th}} = W_q^{\text{th}} n_{q-1} + R_{q+1} n_{q+1} - (W_{q+1}^{\text{th}} + R_q) n_q,$$

$$S_0^{\text{th}} = R_1 n_1 - W_1^{\text{th}} n_0, \quad S_{z_n}^{\text{th}} = W_{z_n}^{\text{th}} n_{z_{n-1}} - R_{z_n} n_{z_n}, \tag{26}$$

$$S = \sum_{q=1}^{z_n} q S_q^{\text{th}} = \sum_{q=1}^{z_n} (W_q^{\text{th}} n_{q-1} - R_q n_q),$$

where W_q^{th} and R_q denote the total frequencies of thermal ionization and recombination, respectively, averaged over energy levels. The ionization and recombination frequencies and the level distribution of ion populations are defined by the plasma composition, temperature, and density and by the parameters of the electromagnetic field irradiating the plasma, namely, the wave intensity and length.

In the case of low electron temperatures (up to 10 eV), the determining processes will be those of optical ionization of matter in the electric field of laser wave decaying in the skin of the target.[2]

Estimation of the role of optical ionization of matter. To obtain a lower estimate of the degree of optical ionization of the surface layer of a target, we will ignore the decrease in the ionization potential in a dense plasma and treat the approximation of isolated atom, the theory of whose ionization is fairly well developed. Such an approximation is justified in the case of multiple ionization of ions with high ionization potentials.

We will use the simple model suggested by Krainov and Manykin [11] for the ionization of medium and heavy atoms in a steady-state electric field. The steady-state field approximation is valid under conditions of tunnel ionization where the electron-potential barrier collision frequency exceeds the ionizing field frequency. In so doing, the Keldysh parameter is $\gamma_K = \omega_0 \sqrt{2mU_q}/eE < 1$, which enables one to substitute the envelope of the intensity of variable field E into the respective formulas for a steady-state field. In the mode of multiphoton ionization with $\gamma_K > 1$, the optical ionization frequency turns out to be higher than it follows for the formulas derived for the mode of tunnel ionization; therefore, the formulas given below will in this case provide a lower estimate for the degree of ionization.

We follow Krainov and Manykin [11] and assume that the electrons being ionized are in the field of "mean" ion with the degree of ionization $\kappa = Z/z_n$ (Z is the ion charge), described by the self-consistent Thomas–Fermi potential U_κ,

$$U_\kappa = \begin{cases} -z_n e^2 \phi(x)/r - Ze^2/r_\kappa, & r < r_\kappa \\ -Ze^2/r, & r > r_\kappa. \end{cases} \tag{27}$$

Here, r_κ is the radius of an ion with the degree of ionization κ and $\phi(x)$ is the solution to the problem

$$\phi'' = \phi^{3/2}/\sqrt{x}, \quad \phi(0) = 1, \quad \phi(X_\kappa) = 0, \quad X_\kappa \phi'(X_\kappa) = -\kappa, \tag{28}$$

where $x = r/b$, $X_\kappa = r_\kappa/b$, $b \equiv (1/2)(3\pi/4)^{2/3} a_B z_n^{-1/3} \approx 4.66 \times 10^{-9} z_n^{-1/3}$ cm, and a_B is the Bohr radius. In the potential given by Eq. (27), the electrons fill the energy states from $-\infty$ to $U_f = -Ze^2/r_\kappa$. In the presence of an electric field with the intensity amplitude E, the potential U_κ changes to the potential $V_\kappa = U_\kappa - erE$, which has a maximum with energy $V_0 = -2e\sqrt{eZE}$. In so doing, all electrons of energy from V_0 to U_f are ionized, with the ionization proceeding until the Fermi energy

[2] Note that the quantity Q_J in formula (3) describes the expenditure of energy on *thermal* ionization of matter, which is zero in the case of optical ionization.

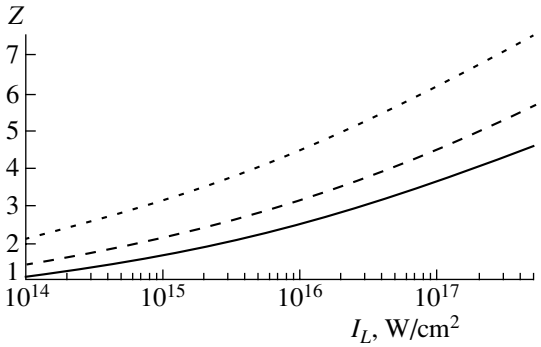

Fig. 2. The average ion charge for a silicon plasma formed in the case of tunnel ionization of the target surface: solid curve, $\lambda_0 = 1.25$ μm; dashed curve, 0.62 μm; dotted curve, 0.2 μm.

U_f becomes equal to V_0. The dimensionless ion radius $X_\kappa = r_\kappa/b$ is found from the condition of equality of U_f and V_0; after that, relations (28) are used to derive the equation for the degree of ionization $\kappa = Z/z_n$. In contrast to [11], we will take into account the fact that, in the plasma of a higher-than-critical concentration forming on the target surface, the field on the interface with vacuum $E(x = +0)$ is approximately $\omega_{pe}/[2\omega_0]$ times lower than the vacuum field $E_L = \sqrt{8\pi I_L/c}$ (in the mode of high-frequency skin effect). As a result, we find that the dimensionless ion radius X_κ and the degree of ionization κ are defined by the equations

$$X_\kappa \approx \sqrt{\kappa^{3/2}/\eta}/2.124, \quad \eta \equiv \breve{I}^{-1/2}\breve{\lambda}^{-1}\breve{n}^{-1}z_n^{-13/6}, \qquad (29)$$

$$2.124\sqrt{\kappa^{1/2}\eta} + \phi'(\sqrt{\kappa^{3/2}/\eta}/2.124) = 0. \qquad (30)$$

In Eqs. (29) and (30), ϕ is found from the solution given by (28) and η is a dimensionless parameter written in the following dimensionless units convenient for what will follow:

$$\breve{\lambda} \equiv \frac{\lambda_0}{1\ \mu\text{m}}, \quad \breve{n} \equiv \frac{n_{\text{at}}}{6\times 10^{22}\ \text{cm}^{-3}},$$
$$\breve{I} \equiv \frac{I_L}{10^{18}\ \text{W/cm}^2}, \quad \breve{T} \equiv \frac{T}{1\ \text{eV}}, \quad \breve{t} \equiv \frac{t}{1\ \text{fs}}. \qquad (31)$$

Figure 2 gives the results of calculation, by formulas (28), (29), and (30), of the average ion charge $Z = \kappa z_n$ for silicon as a function of the energy flux I_L of a laser pulse. The calculations were performed for three wavelengths: 1.25, 0.62, and 0.2 μm.

It follows from Fig. 2 that, at $I_L \sim 10^{14}$ W/cm^2, the average charge of silicon ions is $Z \sim 1$–2, and, at $I_L \sim 10^{17}$ W/cm^2, $Z \sim 3.5$–6.5. The wavelength dependence of Z is in this case associated with the field attenuation coefficient $\omega_{pe}/[2\omega_0]$. At the same time, the quasi-stationary model of thermal ionization discussed in the subsequent section enables one to obtain the same values of the mean ion charge $Z = 1.8$ even at a temperature of the order of 20 eV, and $Z = 6$ at $T = 75$ eV.

Therefore, as the target is heated, the thermal ionization will have a significantly greater effect. In addition, the part played by thermal ionization is especially important deep within the target at a distance from the surface that exceeds the skin depth, where the electric field of laser radiation, along with the probability of optical ionization, goes to zero.

Quasi-stationary model of thermal ionization. When the processes of ionization and recombination are almost compensated, i.e., the rate S_q^{th} of variation of ion concentration with the degree of ionization q turns out to be much lower than both the total ionization rate and the total recombination rate, the quasi-stationary model of ionization $n_q = n_q\{T(t), n_{\text{at}}(t)\}$ may be employed. According to Eqs. (26), this calls for the validity of the inequalities $|W_q^{\text{th}} n_{q-1} - R_q n_q| \ll W_q^{\text{th}} n_{q-1}, R_q n_q$. For this case, we rewrite Eqs. (25) in the form

$$S_q^{\text{th}} \approx (\partial n_q/\partial T)[\partial/\partial t + \mathbf{U}\nabla]T + \text{div}\mathbf{U}[n_q - n_{\text{at}}\partial n_q/\partial n_{\text{at}}],$$

where the values of concentration n_q are determined from the equalities $W_q^{\text{th}} n_{q-1} = R_q n_q$, $q = 1, 2, \ldots, z_n$, to derive from Eqs. (3) and (8) the equation

$$\left(\frac{3}{2} + C_{i1} + C_{i2}\right)n\left[\frac{\partial}{\partial t} + \mathbf{U}\nabla\right]T = -\text{div}q_T + Q_{IB} - (1 + C_3)nT\text{div}\mathbf{U} + Q^{ie},$$
$$C_{i1} = \frac{1}{n}\sum_{q=1}^{z_n}\frac{\partial n_q}{\partial T}\sum_{k=1}^{q} U_k, \quad C_{i2} = \frac{3T}{2n}\sum_{q=1}^{z_n} q\frac{\partial n_q}{\partial T}, \qquad (32)$$
$$C_3 = -\frac{n_{\text{at}}}{Z}\sum_{q=1}^{z_n}\frac{\partial(n_q/n_{\text{at}})}{\partial n_{\text{at}}}\left[\sum_{k=1}^{q}\frac{U_k}{T} + \frac{3}{2}q\right].$$

Used for simplicity in (32) is the equation of state for ideal gas; the small term proportional to $|\mathbf{V}_E|^2 S$ is omitted.

One can see in Eqs. (32) that the coefficients C_{i1} and C_{i2} may be treated as "ionization heat capacities," and the coefficient C_3 is significant only in the regions with $\text{div}\mathbf{U} \neq 0$.

In order to find these coefficients, we must concretely define the form of the dependence $n_q\{T(t), n_{\text{at}}(t)\}$; for this purpose, we take into account the following. The plasma formed on the surface of a target irradiated by a subpicosecond laser pulse is an optically thin medium; i.e., its thickness is much less than the photon path defined by bremal radiation is only emitted, but is not absorbed in the plasma; as a result,

$W_{q+1}^{\text{th}} = n\langle\sigma_{i_q}\mathbf{v}\rangle$ and $R_{q+1} = n^2\langle\sigma_{r_{q+1}}\mathbf{v}_1\mathbf{v}_2\rangle + n\kappa_{d_{q+1}} + n\kappa_{\nu_{q+1}}$, where σ_{i_q} and $\sigma_{r_{q+1}}$ denote the cross sections of impact ionization and triple recombination, respectively, angle brackets indicate averaging over electron velocities, and $\kappa_{d_{q+1}}$ and $\kappa_{\nu_{q+1}}$ are the coefficients of dielectronic and radiation recombination, respectively [12]. The dielectronic recombination may be significant only in the case of a superdense (with a higher-than-solid-state density) plasma [13], and the radiation recombination frequency estimated by Seaton's model [14] is low compared to the three-particle recombination frequency for a high-temperature ($T \gtrsim 10^2$ eV) solid-state plasma. Therefore, we can assume the validity of the inequality $\kappa_{d_{q+1}} + \kappa_{\nu_{q+1}} \gg n\langle\sigma_{i_{q+1}}\mathbf{v}_1\mathbf{v}_2\rangle$, which makes it possible to describe the ionization equilibrium by the Saha model with n_q determined from the equalities

$$n_{q+1}/n_q = (g_{q+1}/g_q)[2/(\lambda\!\!\!^{-3}n)]\exp(-U_{q+1}/T), \quad q = 1, \ldots, z_n. \tag{33}$$

Here, $\lambda\!\!\!^{-} = \hbar\sqrt{2\pi/(mT)}$ is the de Broglie wavelength of electron and g_q is the statistical weight of the ground state of an ion with the degree of ionization q (we ignore the populations of excited states).

In the case of transition from lithium-like to helium-like ion, the ionization potential abruptly increases, and the rate of ionization abruptly decreases; this may limit the validity of the steady-state model. In this case, the forbiddenness of the ionization of helium-like ion is justified, when q in expressions (33) runs from 1 to $z_n - 2$, and the ion concentrations n_{z_n-1} and n_{z_n} are taken to be zero. This model will be referred to as the Saha model with a "cut-off."

The electron temperature dependence of the average ion charge Z, "ionization heat capacities" C_{i1}, C_{i2}, and coefficient C_3, calculated by the Saha model and by the Saha model with a cut-off for an aluminum plasma of solid-state density ($n_{\text{at}} = 6\times10^{22}$ cm^{-3}) is given in Fig. 3.

Kinetic model of thermal ionization. In accordance with the foregoing, we will assume the processes of radiation and dielectronic recombination to be of no significance and treat the unsteady-state plasma dynamics in view of only the collisional ionization and recombination processes. In so doing, we will use the well-known mean ion approximation within which it is assumed that a plasma contains only one sort of ions of concentration n_{at} obeying the continuity equation (1) and continuously varying as a result of ionization by a charge Z. We take into account the three-particle recombination with the aid of the detailed balancing principle and use the semiempirical formula of Lotz [15] for the rate of impact ionization $\kappa_{i_q} = n\langle\sigma_{i_q}\mathbf{v}\rangle$ to

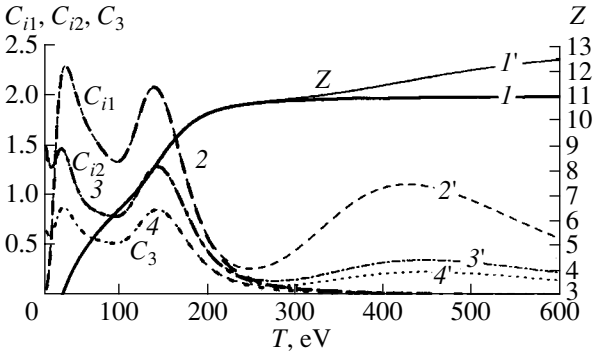

Fig. 3. (*1*, *1'*) The average ion charge Z, ionization heat capacities (*2*, *2'*) C_{i1} and (*3*, *3'*) C_{i2}, and (*4*, *4'*) the coefficient C_3 for an aluminum plasma of solid-state density ($n_{\text{at}} = 6\times10^{22}$ cm^{-3}); (*1'*, *2'*, *3'*, *4'*) Saha model, (*1*, *2*, *3*, *4*) Saha model with a "cut-off."

derive, in view of (1), the equation for the average charge Z [16],

$$\frac{\partial Z}{\partial t} + (\mathbf{U}\nabla)Z = S/n_{\text{at}} = n_{\text{at}}^{-1} \times \sum_{q=1}^{z_n}(n_{q-1}W_q^{\text{th}} - R_q n_q) \approx Z n_{\text{at}}\kappa(Z)\left[1 - \frac{Z}{Z_{\text{eq}}}\right]. \tag{34}$$

In this formula, the average ionization frequency $n_{\text{at}}^{-1}\sum_{q=1}^{z_n} n_{q-1}W_q^{\text{th}}$ is approximately replaced by a function of the average degree of ionization $n\kappa(Z)$, where $n = Zn_{\text{at}}$ and

$$\kappa(Z) \approx 6\times10^8\sum_{n=1}^{3}\xi_n(Z)e^{-U_n/T}\frac{(U_H)}{U_n}\left(\frac{U_H}{T}\right)^{1/2}\phi\left(\frac{U_n}{T}\right),$$

$$\xi_n(Z) = 2n^2\Phi\left(\frac{z_n - P_{n-1} - Z}{2n^2}\right), \tag{35}$$

$$U_n(Z) = (z_n - P_{n-1} - \xi_n(Z) + 1)^2\frac{U_H}{n^2}.$$

In Eqs. (35), the coefficient 6×10^8 has the dimension of cm^3/s; ξ_n is the number of electrons on a shell with the main quantum number n; P_n is the number of electrons in closed electron shells (P_n = 0, 2, 10, 28, … for n = 0, 1, 2, 3, …, respectively); U_n is the effective potential of a shell number n in the "hydrogen" approximation; $\mathcal{Q}(x)$ is a function equal to zero at $x < 0$, to unity at $x > 1$, and to x at $x \in [0; 1]$; and the function of Φ is defined as $\phi(x) \approx \ln\left[1 + \dfrac{1 + 2.5x}{1.78x(1 + 1.4x)}\right]$.

The term with Z/Z_{eq} in the right-hand part of Eq. (34) allows for the three-particle recombination. In so doing, the quantity Z_{eq} denotes an equilibrium aver-

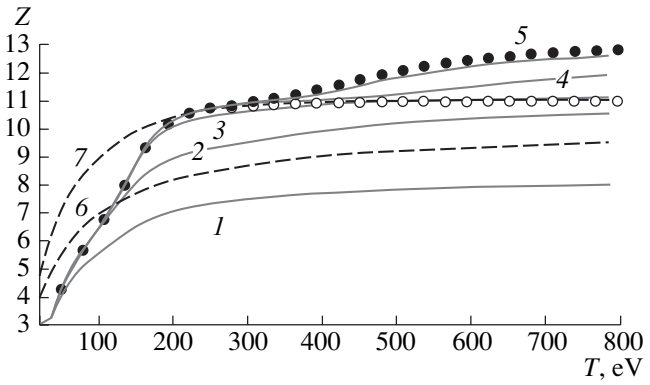

Fig. 4. The average ion charge for a solid-state aluminum plasma ($n_{at} = 6 \times 10^{22}$ cm^{-3}) as a function of temperature: (*1–5*) calculation by the unsteady-state model of mean ion in view of three-particle recombination, (*6*, *7*) calculation disregarding three-particle recombination; the instants of time of (*1*, *6*) 10 fs, (*2*, *7*) 100 fs, (*3*) 1 ps, (*4*) 10 ps, (*5*) 100 ps; lines with black markers indicate the Saha model, lines with white markers indicate the Saha model with a cut-off.

age ion charge; for given plasma temperature and density, this charge is found from the quasi-stationary Saha model given by (33).

We can use Eqs. (34) and (35) to write the following expression for the ionization loss density Q_U (instead of Eq. (8)):

$$Q_U = n_{at}(Zn_{at}\kappa(Z) - \mathbf{U}\nabla Z)\sum_{n=1}^{3}\frac{\partial U_n}{\partial Z},$$

$$\frac{\partial U_n}{\partial Z} = \begin{cases} 2(z_n - P_{n-1} - \xi_n(Z) + 1)\dfrac{U_H}{n^2} \\ \text{for } \dfrac{z_n - P_{n-1} - Z}{2n^2} \in (0;\,1) \\ 0 \text{ for the rest of the cases.} \end{cases} \quad (36)$$

Figure 4 gives comparison of the results of calculation of the average ion charge Z for a solid-state aluminum plasma ($z_n = 13$) by the unsteady-state model of mean ion (34), (35) and by the thermodynamic Saha model with and without a cut-off. Curves *1–5* correspond to the instants of time of 10 fs, 100 fs, 1 ps, 10 ps, and 100 ps, respectively. The calculation results lead one, first, to conclude that the three-particle recombination plays a significant part (compare curves *1*, *2* and *6*, *7*) and, second, to estimate the time required to attain ionization equilibrium at different temperatures. It follows from Fig. 4 that this time will be 10 fs or less for aluminum ions with the degree of ionization from three to five, 10 to 100 fs for ions with the degree of ionization from five to eight, and 100 fs to 1 ps for ions with the degree of ionization from eight to eleven under conditions of fixed temperature and solid-state density. For helium-like and hydrogen-like atoms, the time of relaxation to ionization equilibrium is much longer (about a hundred picoseconds). Analysis of Fig. 4 reveals that, in the case of a plasma of solid-state density at times from 100 fs to several picoseconds, one can use the Saha model with a cut-off; at times longer than ten picoseconds, a uniform distribution arises with the average degree of ionization of the ions defined by the Saha model without a cut-off. For a more rarefied plasma, the time of relaxation to ionization equilibrium increases inversely as the electron concentration of the plasma (see expression (34) for the ionization frequency).

2. ANALYTICAL ESTIMATION OF TARGET HEATING

In order to analytically describe a heat wave propagating in a target, assuming that the laser pulse is not too sharply focused and, therefore, its transverse dimension is much larger than the characteristic dimension of the heat wave, we will treat the simplified one-dimensional equation for the temperature of nondegenerate electron gas

$$(3/2)n\partial T/\partial t = -\partial q_T/\partial x + Q_{IB}, \quad (37)$$

which includes only the basic factor of energy balance, namely, the source of plasma heating Q_{IB} and the heat flux q_T. In solving this equation, we will assume that the total concentration of atoms and ions n_{at} and the average ion charge Z are constant. In order to estimate the effect of hydrodynamic expansion of plasma on the energy contribution made by laser to the target and the effect of the nonlinear dependence of absorption on the laser field intensity [5] in the case of violation of condition (10), we will use the variation factor of absorption κ_A (see Section 1.2). The average ion charge Z will be estimated using the quasi-steady-state models of ionization described in Section 1.3.

In order to determine how close the solution of Eq. (37) may be to that of Eq. (3), we will estimate the ratio of the terms omitted upon transition from Eq. (3) to (37) to $n\partial T/\partial t \sim nT/\tau_T$. Here, τ_T is the characteristic time of ionization of plasma; therefore, for the short pulses being treated, the term $(mV^2/2)S$ may also be always omitted. The term $n(\mathbf{V}\nabla)T/[n\partial T/\partial t]$ is of the order of the ratio x_{sT}/x_T, where $x_{sT} \sim V_s\tau_T$ is the characteristic distance of plasma expansion during the time τ_T, $V_s = \sqrt{ZT/m_{at}}$ is the velocity of sound, and x_T is the characteristic dimension of temperature irregularity. For subpicosecond laser pulses, it follows from the results of appropriate calculations (see the next part of this paper) that $x_{sT} < x_T$; therefore, the contribution by the term $(\mathbf{V}\nabla)T$ to the energy balance in the first approximation may be ignored. The effect of plasma expansion and, consequently, of these terms on the

energy balance is taken into account with the aid of the factor κ_A.

For longer pico- and nanosecond pulses, it is probable that $x_{sT} \sim x_T$ and even $x_{sT} \gg x_T$; therefore, the disregard of the term $(\mathbf{V}\nabla)T$ may bring about a significant error. A similar conclusion holds for the term $nT\mathrm{div}(\mathbf{V})$: $nT\mathrm{div}(\mathbf{V})/[n\partial T/\partial t] \sim \tau_s/\tau_T \sim 1$, where τ_s is the characteristic time of plasma expansion. Therefore, this term is also significant, but only in the plasma corona where $V \neq 0$. With the proviso that $x_{sT}/x_T \ll 1$, the size of the plasma corona is small compared to the size of the heated region; therefore, the effect of expansion (and, consequently, of the indicated terms) on the energy balance may be ignored in the first approximation.

Note that the loss of plasma energy due to bremsstrahlung for the subpicosecond laser pulses being treated may always be ignored, as was done in deriving the hydrodynamic equations, because the time of radiation relaxation estimated as the time of twofold decrease in the plasma temperature due to bremsstrahlung by the model of Zel'dovich and Raizer [17] is $\tau_{\mathrm{rad}} = 47\breve{T}^{1/2}\,\breve{n}^{-1}(Z/10)^{-2}$ ps$\gg t_p$. It follows from [17] that the line radiation, in contrast to the recombination one, may always be ignored in the case when the total area of lines is much less than the area under the Planck curve. The assumption is likely that the line radiation will play a prominent part in the energy balance for heavy elements producing a large number of lines in the region of Planck spectrum [4].

Equation (37) may be simplified if we take into account the fact that the depth of field penetration, i.e., the skin thickness l_s, is much less than the heated region dimension x_T for most of the laser pulse duration except for the initial stage of heating in which the heat wave has not yet propagated beyond the skin. This enables one to include the absorption of laser radiation as the boundary condition for the heat flux on the plasma–vacuum interface rather than in the form of a volume source Q_{IB} [18]. Thus, we arrive at the following problem:

$$\begin{gathered}(3/2)n\partial T/\partial t = -\partial q_T/\partial x,\\ q_T(x=0) = AI_L, \quad q_T(x=\infty) = 0,\end{gathered} \tag{38}$$

where q_T is the x-projection of Spitzer's heat flux (7).

In order to use the approximation formulas which well describe the actual absorption coefficient A (see Section 1.2), we will identify in this coefficient the most pronounced temperature dependence,

$$A = T^{-\mu}C_A\{Z, n_{\mathrm{at}}, \lambda_0, \Lambda\}. \tag{39}$$

Here, μ is a constant and C_A is a coefficient dependent on the average ion charge Z, concentration n_{at}, wavelength λ_0, and Coulomb logarithm Λ. We will ignore the variation of Z, n_{at}, and Λ during the heating of plasma, when formula (39) is used to construct a self-similar solution describing such heating. In order to estimate the effect of the time dependence of the laser pulse intensity, we will represent I_L in the form

$$I_L = I_{\max}(t/\tau_p)^{\beta_I}, \tag{40}$$

where τ_p is the characteristic time of variation of the laser pulse intensity and β_I is a constant.

Because the Coulomb logarithm Λ relatively weakly depends on the electron temperature T, and $Z(T)$ reaches saturation at $T > 200$ eV (see Fig. 4), in solving the set of equations (38) in a first approximation, we assume Z and Λ to be constant. In order to estimate the effect made by the laser field intensity dependence of the absorption coefficient and by the plasma expansion on the obtained solution of the set of equations (38), we will assume that the factor κ_A is likewise constant. In the next approximation, the obtained solution may be used to refine the values of Λ, Z, and κ_A.

In view of the foregoing assumptions, Eqs. (38), (39), and (7) may yield the following solution for the electron temperature:

$$\begin{aligned}T = \Psi(\phi)\left[\frac{\sqrt{\pi^3/2}}{24}\frac{e^4\sqrt{m}}{\kappa_z}\right]^{\frac{2}{4\mu+9}}[I_{\max}(\Lambda/n_{\mathrm{at}})^{1/2}\\ \times C_A\{Z, n_{\mathrm{at}}, \lambda_0, \Lambda\}]^{\frac{4}{4\mu+9}}t^{\frac{2}{4\mu+9}}(t/\tau_p)^{\frac{4\beta_I}{4\mu+9}}.\end{aligned} \tag{41}$$

In Eq. (41), the dimensionless coordinate ϕ is related to the coordinate x along the direction of heat wave propagation as

$$\begin{aligned}x = \phi\left[\frac{3\sqrt{\pi^3/2}}{32}\frac{e^4\sqrt{m}}{\kappa_z}\right]^{-\frac{2+2\mu}{4\mu+9}}\left[\frac{2}{3}I_{\max}n_{\mathrm{at}}^{-\frac{7+2\mu}{5}}Z^{-\frac{9+4\mu}{5}}\right.\\ \left.\times\Lambda^{-\frac{2+2\mu}{5}}C_A\{Z, n_{\mathrm{at}}, \lambda_0, \Lambda\}\right]^{\frac{5}{4\pi+9}}t^{\frac{7+2\mu}{4\mu+9}}(t/\tau_p)^{\frac{5\beta_I}{4\mu+9}},\end{aligned} \tag{42}$$

and the function $\Psi(\phi)$ is the solution to the ordinary differential equation

$$\begin{aligned}\Psi^{5/2}\Psi'' + \frac{5}{2}\Psi^{3/2}\Psi'\\ + \frac{5\beta_I + 7 + 2\mu}{9+4\mu}\phi\Psi' - \frac{4\beta_I + 2}{9+4\mu}\Psi = 0\end{aligned} \tag{43}$$

with the boundary conditions

$$\Psi^{5/2+\mu}\Psi'|_{\phi=0} = -1,$$

$$\int_0^\infty \Psi(\phi)d\phi = \frac{9+4\mu}{9(\beta_I+1)+2\mu}\Psi^{-\mu}(0),$$

where $\Psi' \equiv d\Psi/d\phi$. The second boundary condition replaces the condition $\Psi(x = +\infty) = 0$.

We can use Eqs. (41)–(43) to derive an expression for the amount of absorbed energy of laser radiation

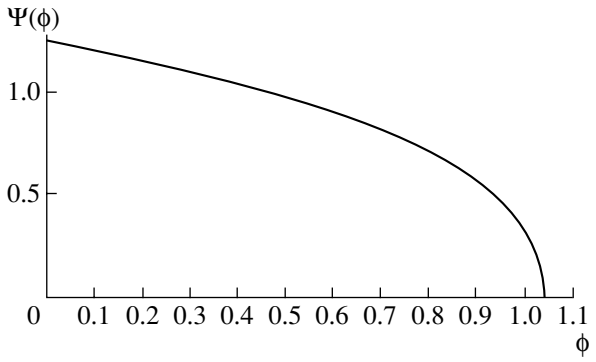

Fig. 5. The self-similar solution $\Psi(\phi)$ for normal skin effect with the approximation coefficient of absorption (24).

(per unit area) $Q_{abs} = \int_0^t A(t) I_L(t) dt$; in the absence of the hydrodynamic, ionization, and other mechanisms of energy redistribution, this expression coincides with that for the energy of electron heat wave (per unit area), $Q_{\text{th}} = (3/2) \times \int_0^\infty n\, T(x) dx$, and has the form

$$Q_{abs} = \Psi(0)^{-\mu} \frac{9 + 4\mu}{9 + 2\mu + 9\beta_I} \left[\frac{\sqrt{\pi^3/2}}{24} \frac{e^4 \sqrt{m}}{\kappa_z} \right]^{-\frac{2\mu}{4\mu + 9}}$$
$$\times [I_{\max} (n_{\text{at}}/\Lambda)^{-2\mu/9} C_A\{Z, n_{\text{at}}, \lambda_0, \Lambda\}]^{9/[4\mu + 9]} \quad (44)$$
$$\times t^{\frac{9 + 2\mu}{4\mu + 9}} (t/\tau_p)^{\frac{9\beta_I}{4\mu + 9}}.$$

Based on Eqs. (43) and (44), we will treat a self-similar solution for a heat wave propagating in an aluminum target. We represent approximation (24) in the form of Eq. (39) to derive from Eqs. (41)–(44) self-similar distributions $T(x, t)$ and $Q_{abs}(t)$,

$$T(x, t) = 157 \Psi(\phi(x)) \kappa_z^{-4/27} (\breve{\kappa}_A \breve{I} Z)^{8/27} t^{4/27}$$
$$\times (\breve{\lambda} \breve{n})^{-2/27} \Lambda^{10/27} (t/\tau_p)^{8\beta_I/27}, \text{ eV},$$
$$x(\phi) = 53 \phi \kappa_z^{17/54} (\breve{\kappa}_A \breve{I})^{10/27} t^{37/54} \breve{\lambda}^{-5/54} n^{-16/27} \quad (45)$$
$$\times Z^{-17/27} \Lambda^{-1/27} (t/\tau_p)^{10\beta_I/27}, \text{ nm},$$

$$Q_{abs} = \frac{5}{5 + 4\beta_I} 1.79 \times 10^8 \kappa_z^{1/6} (\breve{\kappa}_A \breve{I} Z)^{2/3} t^{5/6} \lambda^{-1/6}$$
$$\times (\breve{n} \Lambda)^{1/3} (t/\tau_p)^{2\beta_I/3}, \frac{\text{erg}}{\text{cm}^2}. \quad (46)$$

The self-similar function $\Psi(\phi)$, which is in this case the solution to (43) with $\mu = 9/8$, is shown in Fig. 5 for a square laser pulse ($\beta_I = 0$).

We will treat the restrictions imposed on the range of validity of the derived self-similar solution. The most significant restriction on the laser pulse *duration* is placed by the formation of a plasma corona. The condition that the variation of absorption as a result of expansion is small, so that $\kappa_A \approx 1$ if the dependence of A on the laser field intensity is ignored, is written in the form $x_s \ll l_s$, where $x_s \sim V_s t$, and the skin depth for a normal high-frequency skin effect is $l_s = c/\omega_{pe}$. In combination with the self-similar solution given by (45), this condition leads to the inequality

$$t \ll 10^2 (\breve{\kappa}_A \breve{I})^{-4/29} Z^{-31/29} \breve{\lambda}^{1/29} \breve{n}^{-25/58} \Lambda^{-5/29} M^{1/2}, \text{ fs},$$

in which M is the molar mass of the target matter. One can readily see that this inequality is valid only for times of ten femtoseconds or less. In the case of long times, one must take into account the decrease in the coefficient of collisional absorption because of expansion and set the variation factor of absorption $\kappa_A < 1$. As was mentioned above, at $t_p > 100$ fs, we can assume with good accuracy that $\kappa_A \approx 0.4$. It follows from the solution of (45) and (46) that the plasma expansion causes the most significant decrease in the total absorbed energy of laser radiation Q_{abs} and the target heating depth x_f and a less significant decrease in the target surface temperature $T(x = 0)$.

The main restriction imposed on the *peak intensity* $I_{\max}$ of a laser pulse is associated with the application of the linear theory of skin effect. However, in view of the use of Langdon's correction (11), it is sufficient to require the validity of the inequality $|\mathbf{V}_E|^2 [1 + \nu_{\text{ef}}/\omega_0]^{-2} \leqslant V_{Te}^2$ that is weaker than (10). We treat the mode of normal high-frequency skin effect ($\nu_{\text{ef}} \ll \omega_0$, for simplicity and take into account, in the foregoing inequality, the fact that the field in the plasma is approximately $\omega_{pe}/2\omega_0$ times lower than in vacuum to obtain the condition for the laser pulse intensity in the form $I_L \leqslant cnT/8$. Upon substituting into this inequality the temperature T found from the self-similar solution (45) of the heat equation, we find the following upper bound on the intensity of a square laser pulse:

$$I_{\max} \leqslant 2 \times 10^{17} (t/100)^{4/19} \kappa_A^{8/19} \breve{\lambda}^{-2/19} n^{25/19}$$
$$\times (Z/10)^{35/19} \Lambda^{10/19} (t/\tau_p)^{8\beta_I/19}, \text{ W/cm}^2, \quad (47)$$

where t is in femtoseconds.

As to Langdon's correction (11), its effect on the absorption coefficient is taken into account by the factor κ_A, as was mentioned above.

Note further that formula (7) for the heat flux is valid only in the case of rather low temperature gradients, when the inequality $a_T \lambda_e / x_T \ll 1$ holds, in which λ_e is the electron free path, x_T is the characteristic magnitude of the temperature gradient, and $a_T \approx 50$ is a constant (see [19]). One can demonstrate that this inequality imposes upper bounds on fluxes of the same order as (47). If the condition $a_T \lambda_e / x_T \ll 1$ is invalid, the correlation between the heat flux and the temperature gradient becomes nonlocal and is expressed in the form of convolution of the flux given by Eq. (7) with some core

[19]. However, the results of numerical calculations [3, 10] demonstrate that the nonlocality of the heat flux largely affects the shape of the heat wave by slightly varying its area and the value of temperature on the target surface. For this reason, the inequality $a_T\lambda_e/x_T \ll 1$ is of much less significance than condition (47).

Finally, one must bear in mind that, as follows from Section 1.2 and Fig. 1, the absorption model used in constructing self-similar solutions underestimates the energy contribution at $T \geqslant 1000$ eV (because of disregard of the spatial dispersion) and overestimates the energy contribution at $T < 200$ eV (in a dense nonideal plasma). Nevertheless, comparison with the results of numerical calculations and with experimental data reveals the adequate validity of self-similar solutions in the range of relatively low temperatures $T < 200$ eV as well. According to the experimental data of Fraenkel *et al.* [4], a target of MgF_2 irradiated by a laser pulse with $I_{max} = 3 \times 10^{16}$ W/cm^2, $\lambda_0 = 0.8$ μm, and $t_p = 100$ fs is heated at a depth of 50 nm to a temperature of about 150 eV. At the same time, it follows from the self-similar solution (45) with $\kappa_A = 0.4$, $\Lambda = 3$, and $Z = [Z(\mathrm{Mg}) + 2Z(\mathrm{F})]/3 = 8$ that the target is heated to 150 eV at a depth of 43 nm, which is in good agreement with the experimental data.

Figure 6 gives the results of parametric calculation of the dependence of the target surface temperature both on the wavelength and on the intensity of the square laser pulse acting on the target, performed using both the self-similar solution constructed in this section and self-consistent numerical simulation described in the subsequent section. The calculation was performed for the instant of time $t = 300$ fs, and the recalculation for other instants of time may be approximately performed using the correlation $T \sim t^{4/27}$ (see (45)).[3] In the self-similar solution, the quantities Z and Λ were calculated by iteration with respect to the obtained value of T (two to three iterations produce an accuracy of 5% or better); Z was determined by the Saha model with a cut-off.

Figure 6 demonstrates good agreement between the results of numerical and analytical calculations (dashed contours in Fig. 6) in a wide range of parameters except for the region of relatively low values of intensity, at which a nonideal plasma is formed which exhibits, as was mentioned above, a somewhat overestimated value of the approximation absorption coefficient given by Eq. (24) (see Fig. 1).

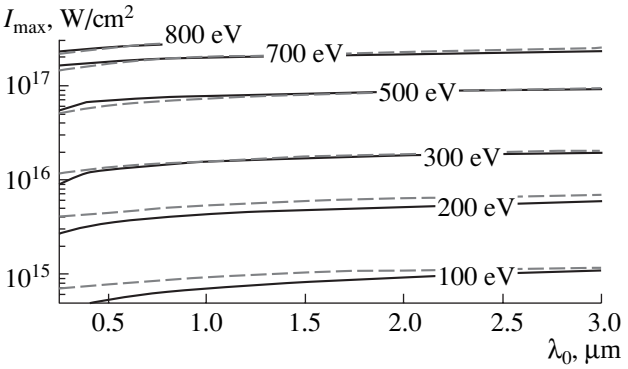

Fig. 6. Lines of the level of temperature of the surface of an aluminum target as a function of wavelength and intensity of square laser pulse for $t = 300$ fs. Solid lines of the level indicate the numerical solution, and dashed lines indicate the self-similar solution (45) with the factor $\kappa_A = 0.4$.

3. RESULTS OF NUMERICAL CALCULATIONS

The self-similar solutions obtained above may be conveniently used to estimate the energy contribution and profile of electron temperature during the time of action of a femtosecond laser pulse. In order to more accurately determine the values of these quantities both during and after the termination of the action of the laser pulse, as well as to determine the characteristics such as the plasma density and pressure, one must numerically solve the foregoing set of equations (1–4), (16) and (33), (34). This problem was treated in a one-dimensional approximation when, as was indicated above, all gradients of physical quantities are directed only along the 0x axis perpendicular to the flat target surface, which presumes the smallness of the characteristic dimensions of the region of localization of the field, of the heat wave, and of the distance to which the plasma expands compared to the transverse dimension of the laser pulse. Hybrid hydroelectrodynamic-ionization one-dimensional computer codes were developed to solve the problem. The hydrodynamic equations (1)–(4) were solved in Lagrangian mass coordinates using a conservative difference scheme [20] with linearization according to Newton and subsequent solution of the respective difference equations by the sweep method. In so doing, splitting with respect to physical processes was employed: the equations of continuity (1) and motion (2) were first solved, followed by the heat equation for electrons (3) and the equation for ions (4). After that, on a preassigned density profile interpolated to a uniform Eulerian grid, the sweep method was used to solve the boundary problem (16) and determine the density of absorbed power of laser radiation; then, the integration of Eq. (34) by the Runge–Kutta method of the fourth order of accuracy was used to determine the ion charge at the next time step and the energy expenditure for the ionization of matter. The accuracy of calculation was checked by calculating the quantity $\Delta \equiv |1 - [Q_{\mathrm{th}} + Q_{\mathrm{th}}^{\mathrm{ion}} + Q_{\mathrm{kin}} + Q_{\mathrm{ioniz}}]/Q_{abs}| \times 100\%$, where Q_{th}, $Q_{\mathrm{th}}^{\mathrm{ion}}$, Q_{kin}, Q_{ioniz}, and Q_{abs} denote the thermal energy of electrons and ions, the kinetic energy of hydrodynamic motion of plasma, the energy expenditure for ionization, and the absorbed energy, respectively. When the quantity Δ exceeded a certain value,

[3] For temperatures of 1 keV or less, when the spatial dispersion may be ignored.

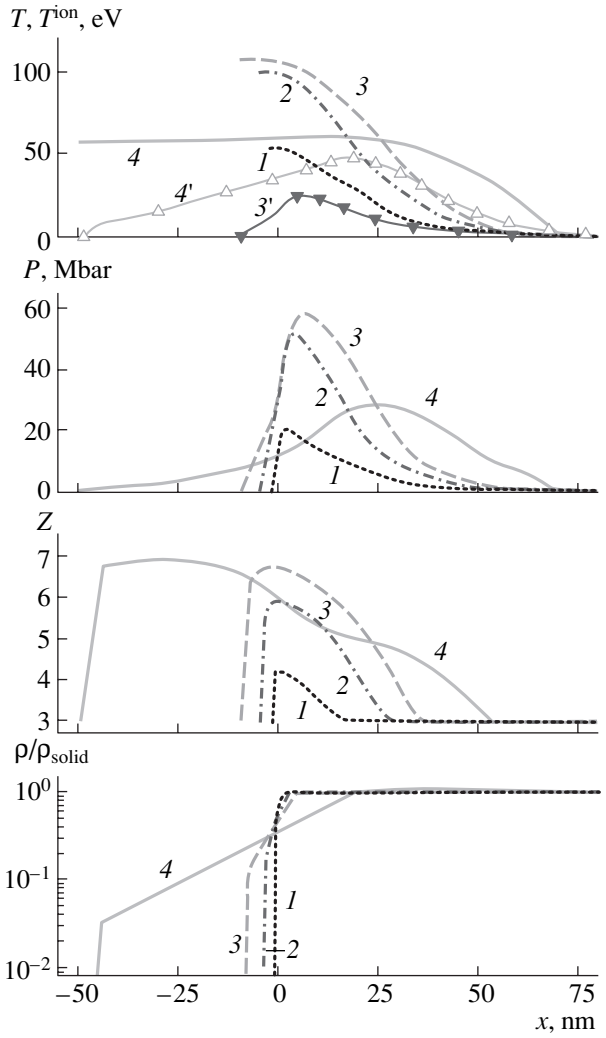

Fig. 7. The distribution, at different instants of time, over the target depth of the hydrodynamic characteristics of the plasma formed when a Gaussian laser pulse 100 fs wide (maximum of the pulse intensity at $t = 0$) affects an aluminum target, $\lambda_0 = 0.1$ μm, $I_{max} = 10^{15}$ W/cm^2: (*1*) $t = -50$ fs, (*2*) $t = 0$ fs, (*3*, *3*') $t = 50$ fs, (*4*, *4*') $t = 300$ fs. In the top drawing: (*1–4*) electron temperature, (*3*', *4*') ion temperature.

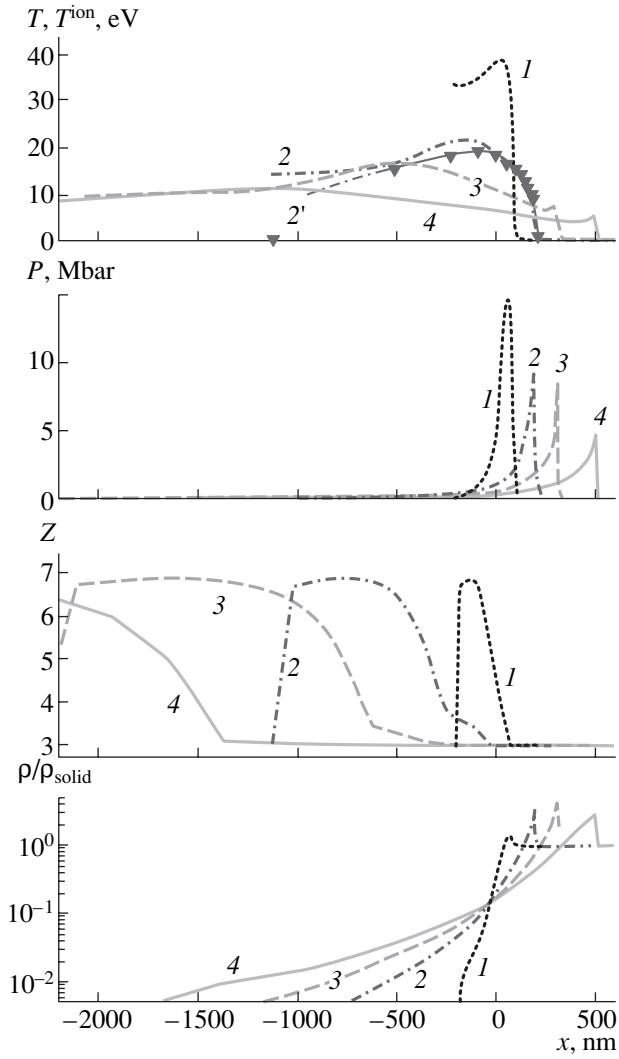

Fig. 8. The same as in Fig. 7, but for different instants of time after the termination of the effect of the laser pulse: (*1–4*) $t = 1$, 5, 10, 20 ps, respectively; (*2*') $t = 5$ ps.

the time step automatically decreased. In the calculations, the value of Δ did not exceed 3%.

An example of numerical solution of the foregoing set of equations in the form of distributions of hydrodynamic characteristics of the plasma being formed over the target depth is illustrated in Fig. 7 for the instants of time when the target is affected by a Gaussian laser pulse with a full width at half maximum of intensity of 100 fs and in Fig. 8 for different instants of time after the termination of the laser pulse action. The laser pulse parameters correspond to those planned for the DESY facility (Germany).

Note that the maximal electron temperature $T_{max} \approx 110$ eV obtained as a result of numerical calculation (Fig. 7) agrees well with the results of self-similar solution (Fig. 6). Note further the high values of pressure in the matter of the target being irradiated throughout the action of the laser pulse. Upon termination of the laser pulse, the heat wave profile spreads out significantly, and the maximal value of temperature decreases (Fig. 8) as a result of the effect of the electron heat conduction, of the plasma expansion, and of the electron–ion relaxation whose effectiveness at low temperatures is much higher than at low temperatures during the time of action of the laser pulse. A shock wave of a characteristic triangular shape forms by the instant of time $t \sim 1$ ps; by the instant of time $t \approx 5$ ps, this shock wave overtakes the heat wave. By the same instant of time, the profiles of electron and ion temperatures for the given parameters of the problem almost level off (Fig. 8).

Figure 9 gives the time dependence of the temperature and concentration of electrons, as well as of the

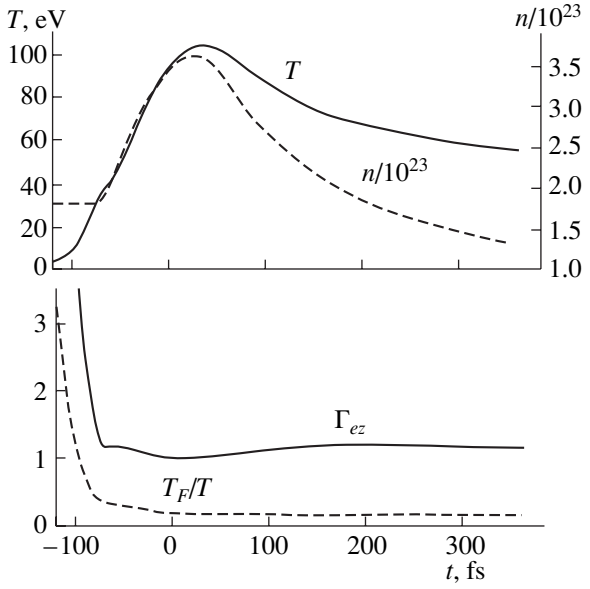

Fig. 9. The time dependence of the temperature and concentration of electrons and of the parameters T_F/T and Γ_{ez} at the target depth x = 5 nm for conditions corresponding to those in Fig. 7.

degeneracy parameter T_F/T and nonideality parameter $\Gamma_{ez} = Ze^2/[n^{-1/3}T]$ of a plasma formed under the effect of a laser pulse at a depth of 5 nm from the surface of the target being irradiated under the same conditions as in Fig. 7. One can see in Fig. 9 that the target matter during most of the laser pulse action is a nondegenerate nonideal plasma with the nonideality parameter $\Gamma_{ez} \approx 1$.

Figure 10 gives the time dependence of the same quantities as those in Fig. 9 but for other parameters of a laser pulse; it is planned to obtain these parameters in the femtosecond laser facility presently under construction at IHED (Institute of High Energy Density, Institute of High Temperatures Scientific Association - IVTAN, Moscow). Based on the foregoing data, one can conclude that a nondegenerate highly nonideal plasma with the parameter $\Gamma_{ez} \gtrsim 2$ is formed on the target surface under the conditions identified above. Therefore, the commissioning of the last-mentioned laser facility is of considerable interest from the standpoint of investigations of the properties of highly nonideal plasma.

In order to provide an idea of the degree of expansion and inhomogeneity of the plasma whose dynamics are shown in Fig. 10, Fig. 11 gives the spatial distribution of hydrodynamic quantities at the instant of time of 300 fs.

CONCLUSIONS

We have suggested simple analytical and numerical models which enable one to investigate the effect of subpicosecond laser pulses on solid-state targets. The constructed self-similar solutions make it possible to fairly accurately estimate the parameters of the heat wave propagating in the target being irradiated during

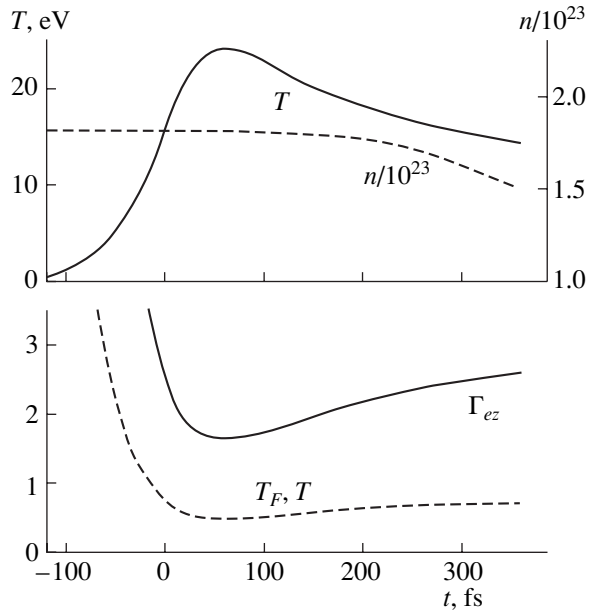

Fig. 10. The time dependence of the temperature and concentration of electrons and of the parameters T_F/T and Γ_{ez} at the aluminum target depth x = 5 nm. The laser pulse is Gaussian, with a width of 100 fs, λ_0 = 1.25 μm, I_{max} = 10^{14} W/cm^2.

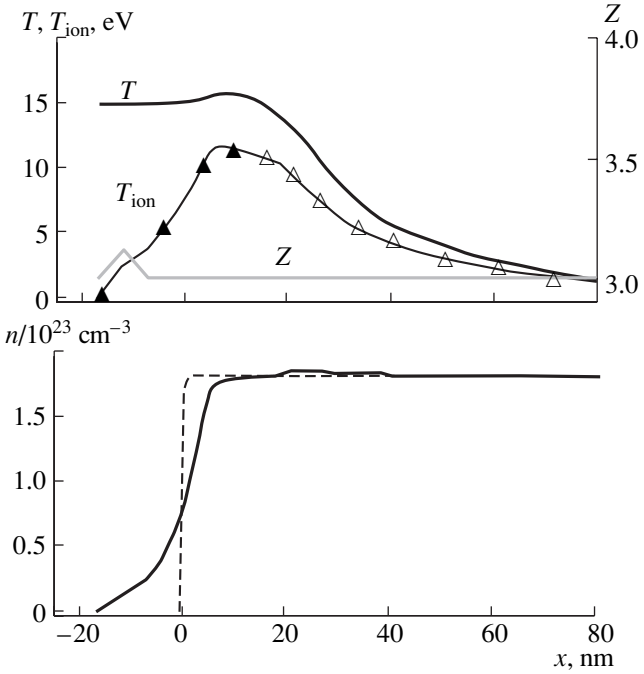

Fig. 11. The distribution of hydrodynamic quantities over the target depth at the instant of time t = 300 fs. The parameters of the problem are the same as in Fig. 10.

the time of action of the laser pulse without resorting to numerical simulation. A more exact calculation of heat wave both during the time of action of the laser pulse and during a much longer time, as well as the calculation of pressure, ionization state, and the degree of expansion of the plasma being formed, may be performed using the computer codes developed for this purpose.

The foregoing models were used to perform preliminary calculations of the effect made on aluminum targets by laser pulses with parameters which it is planned to obtain in the experimental facility presently under construction at IHED and in the DESY facility in Hamburg. In particular, it has been demonstrated that, when a target is affected by a laser pulse with parameters corresponding to those to be obtained at the facility under construction at IHED, a highly nonideal nondegenerate plasma is formed on the target surface, which is of great interest from the standpoint of investigation of the plasma properties.

As the experimental base is further developed, it is planned to compare the models with the results of future experiments and to refine them in the region of highly nonideal plasma.

ACKNOWLEDGMENTS

This study was supported in part by the Russian Foundation for Basic Research, grant nos. 01-02-16 723, and by NATO PST CLG, no. 979372.

REFERENCES

1. Anisimov, S.I., Prokhorov, A.M., and Fortov, V.E., *Usp. Fiz. Nauk*, 1984, vol. 142, p. 395.
2. Arutyunyan, R.V., Baranov, V.Yu., Bol'shov, L.A., *et al.*, *Vozdeistvie lazernogo izlucheniya na materialy* (The Effect of Laser Radiation on Materials), Moscow: Nauka, 1989.
3. Veisman, M.E., Ionization Effects Caused by the Stimulation of Matter by Subpicosecond Laser Pulses, *Cand. Sci. (Phys.-Math.) Dissertation*, Moscow: Institute of High Energy Density, IVTAN (Institute of High Temperatures) Scientific Association, Russian Academy of Sciences, 2002.
4. Fraenkel, M., Zigler, A., Henis, Z. *et al.*, *Phys. Rev. E*, 2000, vol. 61, p. 1899.
5. Langdon, A.B., *Phys. Rev. Lett.*, 1980, vol. 44, p. 575.
6. Yakubov, I.T., *Usp. Fiz. Nauk*, 1993, vol. 163, p. 35.
7. Andreev, N.E., Courtois, C., Cros, B., *et al.*, *Phys. Rev. E*, 2001, vol. 64, p. 016404.
8. Demchenko, N.N. and Rozanov, V.B., A Hydrodynamic Model of Interaction between Picosecond Laser Pulses and Condensed Targets, *Preprint of Inst. of Physics, Russ. Acad. Sci.*, Moscow, 2001, no. 2.
9. Rozmus, W., Tikhonchuk, V.T., and Cauble, R., *Phys. Plasmas*, 1996, vol. 3, p. 360.
10. Andreev, N.E., Kostin, V.V., and Veisman, M.E., *Phys. Scr.*, 1998, vol. 58, p. 468.
11. Krainov, V.P. and Manykin, E.A., *Ukr. Fiz. Zh.*, 1980, vol. 25, p. 400.
12. Vainshtein, L.A., Sobel'man, I.I., and Yukov, E.A., *Vozbizhdenie atomov i ushirenie spektral'nykh linii* (Atomic Excitation and Spectral Line Broadening), Moscow: Nauka, 1979.
13. Salzman, D and Krumbein, A., *J. Appl. Phys.*, 1978, vol. 49, p. 3229.
14. Seaton, M.J., *M. Not. R. Astron. Soc.*, 1959, vol. 119, p. 81.
15. Lotz, W., *Z. Phys.*, 1970, vol. 232, p. 101.
16. Andreev, N.E., Beigman, I.L., Veisman, M.E., *et al.*, Dynamic Models of Ionizing Plasma, *Preprint of Inst. of Phys., Russ. Acad. Sci.*, Moscow, 1998, no. 59.
17. Zel'dovich, Ya.B. and Raizer, Yu.P., *Fizika udarnykh voln i vysokotemperaturnykh gidrodinamicheskikh yavlenii* (The Physics of Shock Waves and High-Temperature Hydrodynamic Phenomena), Moscow: Nauka, 1966.
18. Rozmus, W. and Tikhonchuk, V.T., *Phys. Rev. A*, 1990, vol. 42, p. 7401.
19. Epperlein, E.M. and Short, R.W., *Phys. Fluids B*, 1991, vol. 3, p. 3092.
20. Samarskii, A.A. and Popov, Yu.P., *Raznostnye metody resheniya zadach gazovoi dinamiki* (Difference Methods of Solving Problems in Gas Dynamics), Moscow: Nauka, 1992.